24th INTERNATIONAL CONGRESS ON SOUND AND VIBRATION
23–27 July 2017, London

ICSV24
23-27JULY 2017
LONDON CALLING

INSIGHTS INTO THE GYROSCOPIC BEHAVIOUR OF AXIALLY AND TORSIONALLY LOADED ROTATING SHAFTS

Alessandro De Felice and Silvio Sorrentino

University of Modena and Reggio Emilia, Department of Engineering Enzo Ferrari, Modena, Italy.
email: alessandro.defelice@unimore.it; *silvio.sorrentino@unimore.it*

A distributed parameter model of a straight uniform shaft rotating at constant angular velocity is analytically investigated including the effects of transverse shear, rotatory inertia, gyroscopic moments and considering the additional contribution of combined end thrust and twisting moment. The equations of motion are derived by applying Hamilton's principle according to the Timoshenko beam theory, and cast in dimensionless form to highlight the influence of the main governing parameters (slenderness ratio, angular velocity, applied external end thrust and twisting moment) on natural frequencies and critical speeds of the rotor. The results of this study constitute the basis for further developments, including comparison with finite element models and rotor stability analysis under combined loads.

Keywords: loaded rotating shaft, gyroscopic moment.

1. Introduction

The general increasing trend towards high speed rotating equipment in conjunction with higher power density encourages further insights into the understanding of the dynamic behaviour of torque–transmitting flexible rotors. In this research field the use of finite element models is nowadays widespread, however distributed parameter formulations still remain of some interest, at least for analytical investigations and validation purposes.

Continuous models of rotating shafts have been studied by several researchers who have dealt with many important aspects, highlighting the effects of transverse shear, rotatory inertia, gyroscopic moments and considering the additional contribution of axial end thrust and twisting moment.

The gyroscopic effects were studied considering rotating Timoshenko beams. The equations of motion for symmetric and asymmetric rotors, without the contribution of axial loads, were derived by Dimentberg [1] adopting the Newtonian formulation and later by Raffa and Vatta [2] with Lagrangian formulation via Hamilton's principle.

Early investigations about the effects of axial end thrust and twisting moment of constant magnitude acting simultaneously on a uniform shaft can be found in the works of Greenhill [3] and Southwell and Gough [4], who first considered the influence of these loads on critical speeds.

More recently, the effects of an axial end twisting moment alone on the flexural behaviour of a rotating slender shaft was studied according to the Euler–Bernoulli beam model by Colomb and Rosemberg [5], and according to the Timoshenko beam model by Eshleman and Eubanks [6], who focused their analysis on critical speeds without considering natural frequencies. They found that the Euler–Bernoulli model is inaccurate in predicting the critical speeds, and that the latter always decrease with external axial torque. Following the results by Eshleman and Eubanks, the topic was then again considered, among others, by Lee [7].

The equations of motion of a rotating Timoshenko beam subjected to axial end thrust were derived with Lagrangian formulation by Choi *et al*. [8]. An analysis of the effects of combined external axial end thrust and twisting moment was proposed by Willems and Holzer [9] and later by Dubigeon and Michon [10], who adopted the Timoshenko beam model, casting doubts on some results obtained by Eshleman and Eubanks.

In the present study some further insights are proposed in the analysis of a distributed parameter model of a high–speed, power transmitting flexible rotor. A homogeneous uniform Timoshenko

straight beam with circular section is considered, rotating with constant angular speed about its longitudinal axis on isotropic supports, and subjected simultaneously to constant end thrust and twisting moment. The equations of motion are derived using a variational formulation, and cast in non-dimensional form to facilitate the analysis of the effects of each governing parameter [11].

A study of the influence of slenderness ratio, angular speed, applied axial end thrust, applied axial end twisting moment and of their interactions on natural frequencies and critical speeds is conducted to determine their relative importance.

2. Equations of motion and solution method

The equations of motion are derived in Lagrangian formulation adopting the small strain assumption [8], and decoupled using complex variables. The general integral is sought by separation of variables, via modal analysis, yielding eigenfrequencies, closed–form expressions for the eigenfunctions, and critical speeds.

2.1 Model description and nomenclature

A homogeneous uniform Timoshenko straight beam with circular section is considered, rotating at constant angular speed about its longitudinal axis and simultaneously subjected to axial end thrust and twisting moment. The model is characterized by the following parameters:

$A = \pi r^2$ = cross – sectional area [m^2]
l = length of the shaft [m]
E = Young's modulus [N/m^2]
G = shear elasticity modulus [N/m^2]
$I_y = I_z = J$ = moment of inertia of the cross-section [m^4]
$I_x = 2J$ = polar moment of inertia of the cross-section [m^4]
κ = transverse shear factor
N = axial end thrust [N]
T = axial end twisting moment [Nm]
ν = Poisson's ratio
ρ = density [Kg/m^3]
ω = rotating angular speed [rad/s]

The external loads N (positive if tensile) and T (positive if counterclockwise) are assumed constant with respect to time. Isotropic supports are considered, making the whole model axisymmetric. Hence it can be represented in a non–rotating coordinate system as shown in Fig. 1. Additional nomenclature includes:

u, v, w = displacements in the x, y, z directions [m]
$\vartheta_x, \vartheta_y, \vartheta_z$ = angular displacements about the x, y, z axes [rad]
$\mathrm{w} = v + iw$ = complex displacement [m]
$\theta = \vartheta_z + i\vartheta_y$ = complex angular displacement [rad]

In next sections a simplified notation for partial derivatives is adopted, dots denoting differentiation with respect to time and roman numbers denoting differentiation with respect to x.

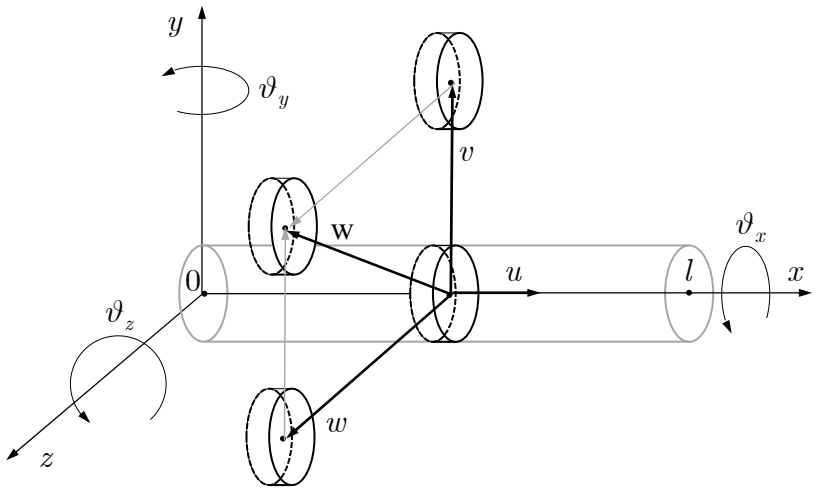

Figure 1: Schematic of the model.

2.2 Lagrangian formulation of the equations of motion

The linear equations of motion of the loaded rotating shaft are obtained by applying Hamilton's principle to the Lagrangian density function $\mathcal{L}$, written associating a work density to the external loads, which are not derivable from a potential:

$$\mathcal{L} = \mathcal{T} - \mathcal{V} + \mathcal{W} \tag{1}$$

where $\mathcal{T}$, $\mathcal{V}$ and $\mathcal{W}$ denote the kinetic energy density, the potential energy density and the work density, respectively. Referring to the nomenclature introduced in Section 2.1, the kinetic energy density takes the form [2][8]:

$$\mathcal{T} = \frac{1}{2}\rho\left[A(\dot{u}^2+\dot{v}^2+\dot{w}^2)+J(\dot{\vartheta}_y^2+\dot{\vartheta}_z^2)+2J\omega^2+2J\omega(\vartheta_z\dot{\vartheta}_y-\vartheta_y\dot{\vartheta}_z)\right] \tag{2}$$

while the potential energy density reads [2][8][12]:

$$\mathcal{V} = \frac{1}{2}\left\{EJ\left[(\vartheta_y^{\mathrm{I}})^2+(\vartheta_z^{\mathrm{I}})^2\right]+\kappa GA\left[(-w^{\mathrm{I}}-\vartheta_y)^2+(v^{\mathrm{I}}-\vartheta_z)^2\right]+EA(u^{\mathrm{I}})^2+2JG(\vartheta_x^{\mathrm{I}})^2\right\} \tag{3}$$

The inclusion of external loads N and T in the Timoshenko beam model is debated in the literature, leading to different forms of the equations of motion [6][8][10][12]. Here the following expression of the work density is adopted:

$$\mathcal{W} = \frac{1}{2}\left\{T(\vartheta_y\vartheta_z^{\mathrm{I}}-\vartheta_y^{\mathrm{I}}\vartheta_z)-N\left[(v^{\mathrm{I}})^2-(v^{\mathrm{I}}-\vartheta_z)^2+(w^{\mathrm{I}})^2-(-w^{\mathrm{I}}-\vartheta_y)^2\right]\right\}+[\delta(x-l)-\delta(x)][Nu+T\vartheta_x] \tag{4}$$

where $\delta(\cdot)$ represents the Dirac distribution, and the contribution of N to flexural vibrations is given accordingly with [8], ensuring consistency with the Timoshenko beam model. Introducing Eqs. (1) to (4) in Lagrange's equations for a continuous one–dimensional problem:

$$\frac{\partial}{\partial t}\left(\frac{\partial\mathcal{L}}{\partial\dot{q}_i}\right)+\frac{\partial}{\partial x}\left(\frac{\partial\mathcal{L}}{\partial q_i^{\mathrm{I}}}\right)-\frac{\partial\mathcal{L}}{\partial q_i}=0, \quad \mathbf{q}=\left\{u,v,w,\vartheta_x,\vartheta_y,\vartheta_z\right\}^{\mathrm{T}} \tag{5}$$

yields the six equations of motion in the form:

$$\begin{cases} \rho A\ddot{u}-EAu^{\mathrm{II}}-[\delta(x-l)-\delta(x)]N=0 \\ \rho A\ddot{v}-\kappa GA\left(v^{\mathrm{II}}-\vartheta_z^{\mathrm{I}}\right)-N\vartheta_z^{\mathrm{I}}=0 \\ \rho A\ddot{w}-\kappa GA\left(w^{\mathrm{II}}+\vartheta_y^{\mathrm{I}}\right)+N\vartheta_y^{\mathrm{I}}=0 \end{cases} \quad \begin{cases} 2\rho J\ddot{\vartheta}_x-2GJ\vartheta_x^{\mathrm{II}}-[\delta(x-l)-\delta(x)]T=0 \\ \rho J\ddot{\vartheta}_y+2\rho J\omega\dot{\vartheta}_z+\kappa GA\left(w^{\mathrm{I}}+\vartheta_y\right)-EJ\vartheta_y^{\mathrm{II}}-T\vartheta_z^{\mathrm{I}}-N\left(w^{\mathrm{I}}+\vartheta_y\right)=0 \\ \rho J\ddot{\vartheta}_z-2\rho J\omega\dot{\vartheta}_y-\kappa GA\left(v^{\mathrm{I}}-\vartheta_z\right)-EJ\vartheta_z^{\mathrm{II}}+T\vartheta_y^{\mathrm{I}}+N\left(v^{\mathrm{I}}-\vartheta_z\right)=0 \end{cases} \tag{6}$$

The first and fourth of Eqs. (6) are decoupled, representing the well known x–direction translational and rotational dynamic equilibrium equations respectively.

Introducing the complex displacements w and θ, the four equilibrium equations describing the flexural behaviour in Eqs. (6) can be decoupled into two fourth–order partial derivative equations with complex coefficients:

$$EJ\left(\mathrm{w}^{\mathrm{IV}}-\frac{\rho}{\kappa G}\ddot{\mathrm{w}}^{\mathrm{II}}\right)-iT\left(\mathrm{w}^{\mathrm{III}}-\frac{\rho}{\kappa G}\ddot{\mathrm{w}}^{\mathrm{I}}\right)-N\psi\mathrm{w}^{\mathrm{II}}+\rho A\psi\ddot{\mathrm{w}}-\rho J\left(\ddot{\mathrm{w}}^{\mathrm{II}}-\frac{\rho}{\kappa G}\ddot{\ddot{\mathrm{w}}}\right)+2i\rho J\omega\left(\dot{\mathrm{w}}^{\mathrm{II}}-\frac{\rho}{\kappa G}\ddot{\mathrm{w}}\right)=0, \quad \psi=1-\frac{N}{\kappa GA} \tag{7}$$

The equation for the complex angular displacement θ is exactly the same, after substituting w with θ. In Eq. (7) complex coefficients identify the terms responsible for coupling the flexural behaviour in the x–y and x–z planes. Notice that Eq. (7) would retain the same form also in the case of an external twisting moment T applied tangentially at the ends of the shaft (i.e. a follower torque) [7]. It generalizes the expression given in [6] (effect of T) and in [8] (effect of N). The equation published in [10] is different, because the effects of N and T where introduced consistently with the Euler–Bernoulli model, rather than with the Timoshenko one.

2.3 Nondimensional form of the equations of motion

The equation of motion (7) is rewritten in nondimensional form to facilitate the analysis of the effects of each governing parameter. Considering a dimensionless spatial variable ξ, a dimensionless time τ, a reference frequency parameter Ω (representing the structural properties of the shaft) along with four dimensionless parameters:

$$\xi=\frac{x}{l},\quad \tau=\Omega t,\quad \Omega=\frac{1}{l^2}\sqrt{\frac{EJ}{\rho A}},\quad \alpha=l\sqrt{\frac{A}{J}}=\frac{2l}{r},\quad \sigma=\frac{E}{\kappa G},\quad \hat{N}=\frac{N}{EA},\quad \hat{T}=\frac{Tl}{EJ} \tag{8}$$

where α is the slenderness ratio of the shaft, then Eq. (7) can be rewritten in nondimensional form as:

$$\left(\mathrm{w}^{\mathrm{IV}}-\frac{\sigma}{\alpha^2}\ddot{\mathrm{w}}^{\mathrm{II}}\right)-i\hat{T}\left(\mathrm{w}^{\mathrm{III}}-\frac{\sigma}{\alpha^2}\ddot{\mathrm{w}}^{\mathrm{I}}\right)-\hat{N}\alpha^2\psi\,\mathrm{w}^{\mathrm{II}}+\psi\ddot{\mathrm{w}}-\frac{1}{\alpha^2}\left(\ddot{\mathrm{w}}^{\mathrm{II}}-\frac{\sigma}{\alpha^2}\ddot{\mathrm{w}}^{\mathrm{II}}\right)+\frac{2i}{\alpha^2}\frac{\omega}{\Omega}\left(\dot{\mathrm{w}}^{\mathrm{II}}-\frac{\sigma}{\alpha^2}\ddot{\mathrm{w}}\right)=0,\quad \psi=1-\sigma\hat{N} \tag{9}$$

For a homogeneous shaft made of isotropic material with circular section, the shear elasticity modulus G and the shear factor κ can be expressed as funtions of Young's modulus and Poisson's ratio [13]:

$$G=\frac{E}{2(1+\nu)},\quad \kappa=\frac{6(1+\nu)}{7+6\nu}\quad\Rightarrow\quad \sigma=\frac{7+6\nu}{3} \tag{10}$$

hence the dimensionless parameter σ depends on Poisson's ratio only, and within the limits of interest for the present study its variations are of minor importance. As a consequence, Eq. (9) depends on four parameters of major interest: slenderness ratio α, dimensionless angular speed ω/Ω, dimensionless axial thrust $\hat{N}$ and dimensionless twisting moment $\hat{T}$ [11].

2.4 Differential eigenproblem

The general integral is obtained via modal analysis, solving a differential eigenproblem. Separating the variables and Laplace transforming with respect to time, Eq. (9) is rewritten in the form:

$$\begin{aligned}&\mathrm{w}(\xi,\tau)=\phi(\xi)\eta(\tau)\quad\Rightarrow\quad \mathrm{L}(\mathrm{w})=\phi(\xi)\eta(s)\quad\Rightarrow\quad p_4\phi^{\mathrm{IV}}+p_3\phi^{\mathrm{III}}+p_2\phi^{\mathrm{II}}+p_1\phi^{\mathrm{I}}+p_0\phi=0\\&\text{with}\quad p_4=1,\quad p_3=-i\hat{T},\quad p_2=-\left[\frac{1+\sigma}{\alpha^2}s^2-\frac{2i}{\alpha^2}\frac{\omega}{\Omega}s+\hat{N}\alpha^2\psi\right],\quad p_1=i\hat{T}\frac{\sigma}{\alpha^2}s^2,\quad p_0=s^2\left(\frac{\sigma}{\alpha^4}s^2-2i\frac{\omega}{\Omega}\frac{\sigma}{\alpha^4}s+\psi\right)\end{aligned} \tag{11}$$

where p_2, p_1 and p_0 depend on the eigenvalue s. The general integral of Eq. (11) can be expressed on the basis of the complex exponential function, yielding a characteristic equation (for the exponents a) with complex coefficients:

$$\phi(\xi)=Be^{a\xi},\quad B,a\in\mathbb{C}\quad\Rightarrow\quad P(a)=p_4a^4+p_3a^3+p_2a^2+p_1a+p_0=0 \tag{12}$$

a quartic polynomial which can be solved symbolically. The general integral is therefore expressed as a linear combination of four complex exponential functions:

$$\phi(\xi)=B_1e^{a_1\xi}+B_2e^{a_2\xi}+B_3e^{a_3\xi}+B_4e^{a_4\xi} \tag{13}$$

and the eigevalues s can be computed after setting four boundary conditions. Assuming the same conditions at both ends of the shaft, the algebraic eigenproblem related to Eq. (11) takes the form:

$$\begin{bmatrix}b_1 & b_2 & b_3 & b_4\\ c_1 & c_2 & c_3 & c_4\\ b_1e^{a_1} & b_2e^{a_2} & b_3e^{a_3} & b_4e^{a_4}\\ c_1e^{a_1} & c_2e^{a_2} & c_3e^{a_3} & c_4e^{a_4}\end{bmatrix}\begin{bmatrix}B_1\\B_2\\B_3\\B_4\end{bmatrix}=\mathbf{0} \tag{14}$$

where the first two equations represent the conditions in $\xi = 0$, and the following two the conditions in $\xi = 1$. The complex valued coefficients b and c depend on the kind of boundary conditions, and in the more general case they are explicit functions of both the exponents a and the eigevalues s. Setting to 0 the determinant of the coefficient matrix in Eq. (14) yields the characteristic equation [11]:

$$\Delta=D_{12}D_{34}\left[e^{a_1+a_2}+e^{a_3+a_4}\right]-D_{13}D_{24}\left[e^{a_1+a_3}+e^{a_2+a_4}\right]+D_{14}D_{23}\left[e^{a_1+a_4}+e^{a_2+a_3}\right]=0,\quad D_{nm}=b_nc_m-b_mc_n \tag{15}$$

which is a complex function of the complex variable s. However, pure imaginary eigenvalues, i.e. $s = i\lambda$, can be numerically computed by using a zero–find routine of a real function f in the real variable λ:

$$f[\Delta(i\lambda)]=0,\quad \lambda\in(-\infty,+\infty) \tag{16}$$

Finally, the critical speeds can be found following the same procedure, setting $\lambda = \omega/\Omega$ in Eq. (16) and solving it with respect to ω.

2.5 Boundary conditions

Isotropic supports are considered, hence the boundary conditions can be expressed as functions of the complex variable w due to axial symmetry. In the simplest configurations they read:

$$\text{Clamped end (long bearings)} \quad \begin{cases} \mathrm{w} = 0 \\ \mathrm{w}^{\mathrm{I}} = 0 \end{cases} \tag{17}$$

$$\begin{matrix} \text{Pinned end (short bearings)} \\ \text{Case with } T = 0 \text{ or with tangential } T \end{matrix} \quad \begin{cases} \mathrm{w} = 0 \\ \mathrm{w}^{\mathrm{II}} = 0 \end{cases} \tag{18}$$

$$\begin{matrix} \text{Pinned end} \\ \text{Case with axial } T \end{matrix} \quad \begin{cases} \mathrm{w} = 0 \\ \mathrm{w}^{\mathrm{II}} - i\hat{T}\,\mathrm{w}^{\mathrm{I}} - \dfrac{\sigma}{\psi\alpha^2}\left[i\hat{T}\left(\mathrm{w}^{\mathrm{III}} - \dfrac{\sigma}{\alpha^2}\ddot{\mathrm{w}}^{\mathrm{I}} - i\hat{T}\,\mathrm{w}^{\mathrm{II}} - \psi\hat{N}\alpha^2\,\mathrm{w}^{\mathrm{I}} \right) - \dfrac{1}{\alpha^2}(\ddot{\mathrm{w}}^{\mathrm{II}} - 2i\hat{\omega}\,\dot{\mathrm{w}}^{\mathrm{II}}) \right] = 0 \end{cases} \tag{19}$$

$$\text{Free end} \quad \begin{cases} \left(\mathrm{w}^{\mathrm{II}} - \dfrac{\sigma}{\alpha^2}\ddot{\mathrm{w}} \right) - i\hat{T}\,\mathrm{w}^{\mathrm{I}} - \psi\hat{N}\alpha^2\,\mathrm{w} = 0 \\ \left(\mathrm{w}^{\mathrm{III}} - \dfrac{\sigma}{\alpha^2}\ddot{\mathrm{w}}^{\mathrm{I}} \right) - i\hat{T}\left(\mathrm{w}^{\mathrm{II}} - \dfrac{\sigma}{\alpha^2}\ddot{\mathrm{w}} \right) - \psi\hat{N}\alpha^2\,\mathrm{w}^{\mathrm{I}} - \dfrac{1}{\alpha^2}(\ddot{\mathrm{w}}^{\mathrm{I}} - 2i\hat{\omega}\,\dot{\mathrm{w}}^{\mathrm{I}}) = 0 \end{cases} \tag{20}$$

Introducing Eq. (13) into the selected boundary equations gives the expressions of the coefficients *b* and *c* in the characteristic equation (15). Notice that the second of Eqs. (19) generalizes the expression given in [6] (with opposite sign convention for T), while in [10] the terms in square brackets are omitted, as a consequence of disregarding the interaction between shear effect and twisting moment in the equations of motion.

3. Discussion of the results

The effects of slenderness ratio α, angular speed ω/Ω, axial end thrust $\hat{N}$ and twisting moment $\hat{T}$ are studied on natural frequencies and critical speeds of the rotating shaft.

3.1 Natural frequencies

Natural frequencies are computed according to the procedure described in Section 2.4, through Eqs. (15) and (16). In the case $\omega = 0$, the absolute value of $\Delta(i\lambda)$ is a symmetric function of the dimensionless parameter λ. Increasing the modulus of $\hat{T}$ (positive or negative) reduces the modulus of natural frequencies λ, as shown in Fig. 2 (left). The same qualitative effect can be observed by increasing the modulus of a negative $\hat{N}$ (compression), and the opposite by raising a positive $\hat{N}$ (traction). In the case $\omega \neq 0$, the former symmetry is lost, and two spectra of natural frequencies are generated by considering $\pm i\lambda$. Increasing ω/Ω with $\omega > 0$, raises the natural frequencies λ as displayed in Fig. 2 (right). Increasing the modulus of ω/Ω with $\omega < 0$, causes the opposite (symmetric) effect.

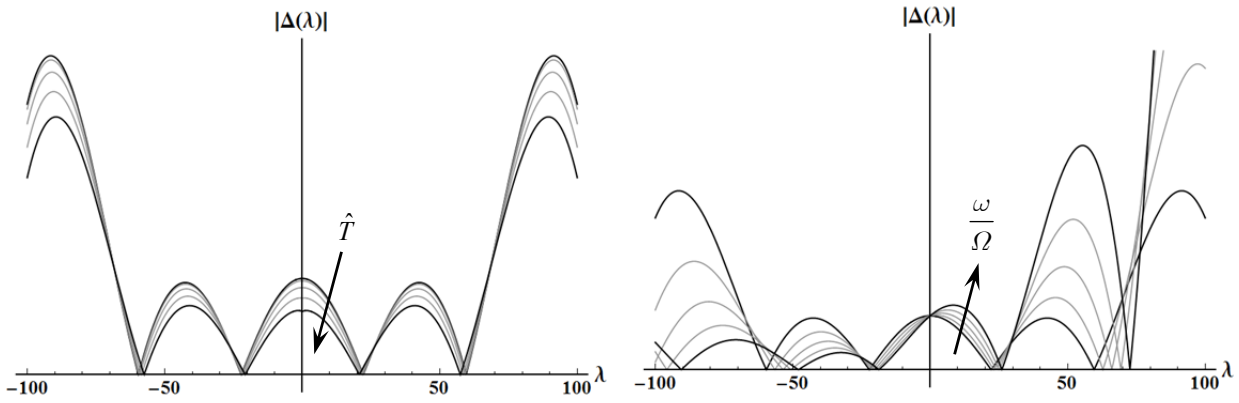

Figure 2. Absolute values $|\Delta(\lambda)|$ of the characteristic function ($\alpha = 50$, $\nu = 0.3$, clamped ends). Left: curves for $\hat{T} > 0$, $\omega/\Omega = 0$, $\hat{N} = 0$. Right: curves for $\omega/\Omega > 0$, $\hat{N} = 0$, $\hat{T} = 0$.

Considering now a simply supported rotating shaft with the following parameters:

$$\rho = 7700\ [\mathrm{Kg/m^3}],\ E = 210\times10^9\ [\mathrm{Pa}],\ \nu = 0.3,\ r = 10\ [\mathrm{mm}],\ l = 250\ [\mathrm{mm}],\ \omega = 1000\ [\mathrm{rad/s}],\ \kappa = 0.8864,\ N = 0,\ T = 0$$

the first 4 natural frequencies $\lambda\Omega$ of the two spectra, computed for the distributed parameter model (DPM) according to the method presented in Section 2.4, are reported in Tab. 1 (α = 50, simply supported shaft) where they are compared with the results of a finite element analysis (FEA) using different numbers of Timoshenko rotating beam elements [11].

Table 1: first 4 natural frequencies $\lambda\Omega$ [Hz] for a rotating unloaded simply supported shaft (short bearings).

	$\omega > 0$				$\omega < 0$			
	FEA – number of elements			DPM	FEA – number of elements			DPM
	1	5	10		1	5	10	
1	736.030	652.037	651.882	651.847	726.306	650.833	650.658	650.6243
2	3351.66	2561.21	2552.27	2550.21	3330.78	2556.56	2547.73	2545.68
3	–	5652.63	5565.59	5544.83	–	5611.01	5556.45	5535.76
4	–	9931.85	9540.54	9440.12	–	9737.23	9526.28	9426.22

Some insights regarding modal shapes come from a qualitative analysis of the four exponents a in Eq. (12). Their dependency on the natural frequencies λ is shown in Fig. 3, for a rotating shaft with α = 10, ω/Ω = 50, $\hat{N}$ = 0.005, $\hat{T}$ = 0 and ν = 0.3. It can be observed that outside a certain interval of λ values, say [λ_b, λ_f], all the exponents become pure imaginary. The two values λ_b and λ_f can be computed as the roots of:

$$P(\lambda) = \lambda^2 - 2\frac{\omega}{\Omega}\lambda - \frac{\alpha^4}{\sigma}\psi \tag{21}$$

For non–rotating unloaded Timoshenko beams, the unique value $\lambda = \alpha^2/\sqrt{\sigma}$ is sometimes referred to as cut–off frequency [14], while Eq. (21) generalizes this concept to the rotating and axially loaded case. Inside the interval (λ_b, λ_f), modal shapes can be defined by combinations of hyperbolic and trigonometric functions; otherwise they are represented by trigonometric functions only.

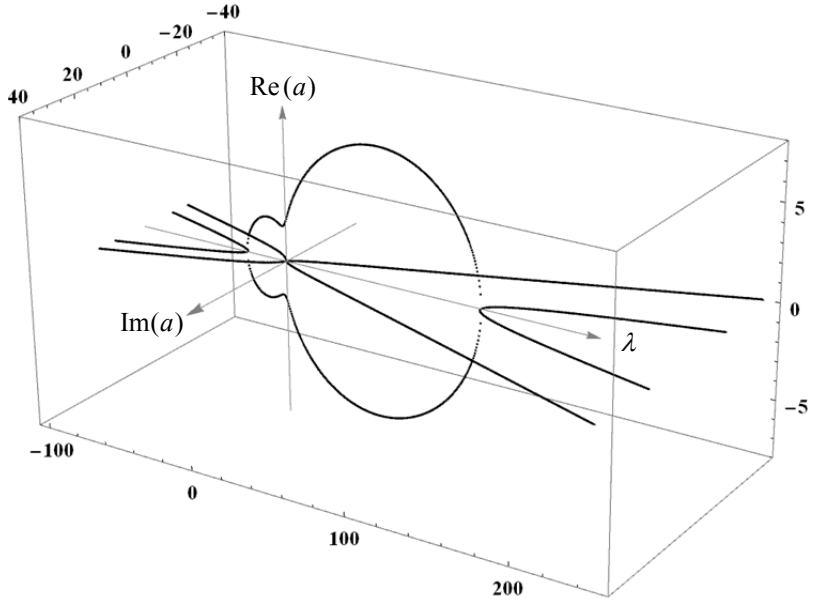

Figure 3. The four roots of Eq. (12), exponents of the modal shapes, as functions of natural frequencies λ.

3.2 Critical speeds

Critical speeds are computed according to the procedure described in Section 2.4, through Eqs. (15) and (16). Campbell 3D diagrams can be drawn, highlighting the influence of a third parameter (say p), other than natural frequencies λ and rotating angular speeds ω/Ω.

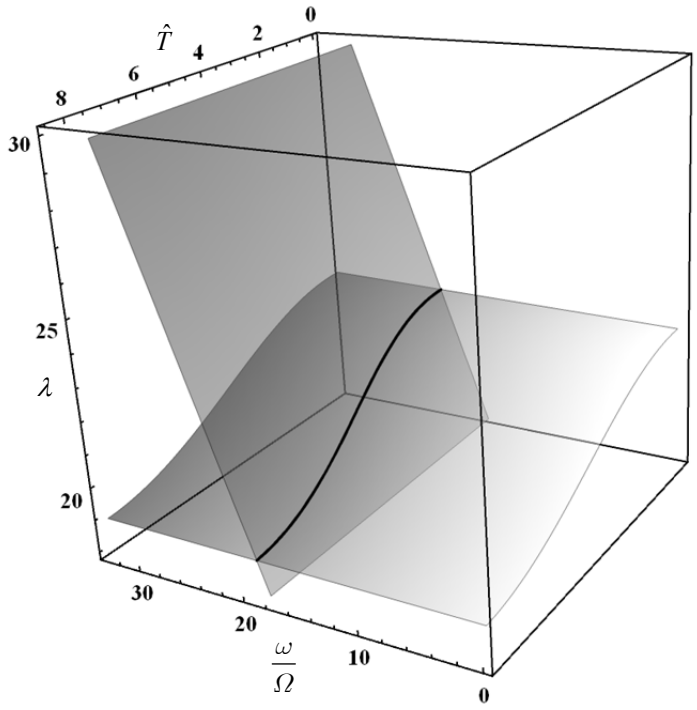

Figure 4. Campbell 3D diagram, first forward critical speed.

The *n*–th nondimensional critical speed $\hat{\omega}_C = \omega_C / \Omega$ is represented by a curve obtained by intersection of the surface associated to the *n*–th natural frequency $\lambda = \lambda\,(\omega/\Omega, p)$ with the plane $\lambda = \omega/\Omega$. For instance, the curve representing the first forward critical speed $\hat{\omega}_{1C}$ of a rotating shaft with $\alpha = 50$, $\hat{N} = 0$, $\nu = 0.3$ and clamped ends (long bearings) is shown in Fig. 4 as a function of $p = \hat{T}$ (where the domain of $\hat{T}$ has been extended up to unrealistic values to test the robustness of computational algorithms).

However, the effects of the main governing parameters on critical speeds are better highlighted by the diagrams displayed in Fig. 5. There the square root of the first nondimensional forward critical speed $\sqrt{\hat{\omega}_{1C}}$ of a rotating shaft with $\nu = 0.3$ and clamped ends (long bearings) is represented as a function of the slenderness ratio α, for different values of $\hat{T}$ in combination with $\hat{N} = 0$ (left), $\hat{N} > 0$ (center) and $\hat{N} < 0$ (right).

Increasing the modulus of $\hat{T}$ always lowers the critical speeds. If $\hat{N} = 0$, then $\hat{\omega}_{1C}$ shows an asymptotic behaviour towards the first nondimensional natural frequency of a slender beam (dotted line in Fig. 4: $\sqrt{\hat{\omega}_{1C}} = 4.730$ [15]), since increasing α the Timoshenko model tends to the Euler–Bernoulli one. The case of traction ($\hat{N} > 0$) produces a stiffening effect on the shaft, raising its critical speeds. The case of compression ($\hat{N} < 0$) causes the opposite effect.

4. Conclusions

A fast and easy to implement method has been proposed for the calculation of natural frequencies and critical speeds of a continuous rotating shaft, consisting of a homogeneous uniform Timoshenko straight beam, rotating at constant angular speed about its longitudinal axis and simultaneously subjected to axial end thrust and twisting moment.

The effects of varying the governing parameters of the model have been studied on natural frequencies and critical speeds, confirming some results found in the literature. Increasing the modulus of twisting moment has the effect of reducing the modulus of both natural frequencies and critical speeds. While the effects of an additional axial end thrust depend on its sign (positive for traction and negative for compression). A positive thrust raises the modulus of both natural frequencies and critical speeds, a negative one lowers them. The so–called cut–off frequencies of the Timoshenko beam model, on the other hand, have been found to depend on the rotating angular speed and on the external loads.

The results of this study constitute the basis for further developments, including comparison with finite element models and rotor stability analysis under combined loads.

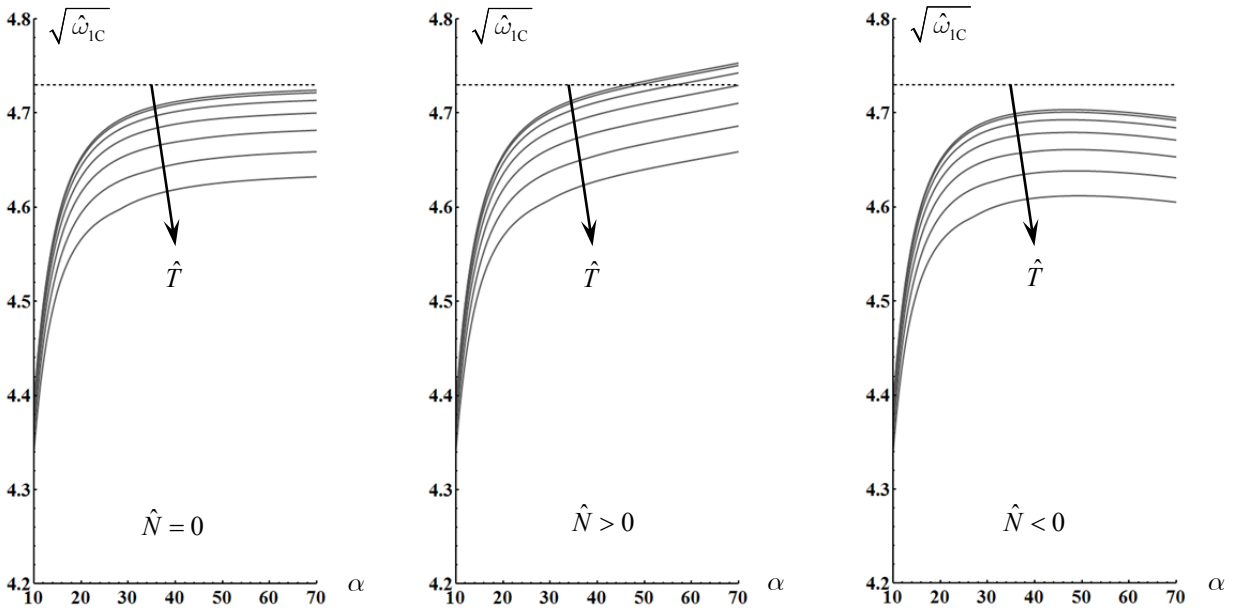

Figure 5: First forward critical speed $\sqrt{\hat{\omega}_{1C}}$ as a function of the slenderness ratio α for different values of $\hat{T}$.

REFERENCES

1 Dimentberg, F.M. *Flexural vibrations of rotating shafts*, Butterworth, London (1961).

2 Raffa, F., Vatta, F. Gyroscopic effect analysis in the lagrangian formulation of rotating beams, *Meccanica*, **34**, 357–366 (1999).

3 Greenhill, A.G. On the strength of shafting when exposed both to torsion and to end thrust, *Proceedings of the Institution of Mechanical Engineers London* **6**, 182–209 (1883).

4 Southwell. R.V., Gough, B.S. On the stability of rotating shaft, subjected simultaneously to end thrust and twist, *British Association for Advancement of Science,* 345 (1921).

5 Colomb, M., Rosemberg, R.M. Critical speeds of uniform shafts under axial torque, *Proceedings of the First U.S. National Congress of Applied Mechanics*, 103–110, New York, USA (1951).

6 Eshleman, R.L., Eubanks, R.A. On the critical speeds of a continuous rotor, *Transactions of the American Society of Mechanical Engineers*, *Journal of Engineering for Industry* **91** / 4, 1180–1188 (1969).

7 Lee, C.W. *Vibration analysis of rotors*, Kluwer, Dordrecht (1993).

8 Choi, S.H., Pierre, C., Ulsoy, A.G. Consistent modeling of rotating Timoshenko shafts subject to axial loads, *ASME Journal of Vibration and Acoustics* **114**, 249–259 (1992).

9 Willems, N., Holzer, S. Critical speeds of rotating shafts subjected to axial loading and tangential torsion, *Transactions of the ASME*, *Journal of Engineering for Industry* **89**, 259–264 (1967).

10 Dubigeon, S., Michon, J.C. Gyroscopic behaviour of stressed rotating shafts, *Journal of Sound and Vibration* **42** / 3, 281–293 (1975).

11 De Felice, A. *Sviluppo di un algoritmo per l'analisi modale computazionale di rotori ad altà velocità* (*Development of an algorithm for computational modal analysis of high–speed rotors*), Master of Mechanical Engineering Thesis, University of Modena and Reggio Emilia (2016).

12 Raffa, F., Vatta, F. Dynamic instability of axially loaded shafts in the Mathieu map, *Meccanica*, **42**, 347–553 (2007).

13 Cowper, G.R. The shear coefficient in Timoshenko's beam theory, *Journal of Applied Mechanics* **33** / 2, 335–340 (1966).

14 Stephen, N.G. The second spectrum of Timoshenko beam theory–further assessment, *Journal of Sound and Vibration* **297**, 1082–1087 (2006).

15 Blevins, R.D. *Formulas for natural frequency and mode shape*, Van Nostrand, New York (1979).